

Published in final edited form as:

*J Med Chem.* 2011 October 13; 54(19): 6647–6656. doi:10.1021/jm200521a.

## Bisphosphonamidate Clodronate Prodrug Exhibits Potent Anticancer Activity in Non-Small Cell Lung Cancer cells

Marie R. Webster<sup>1</sup>, Ming Zhao<sup>2</sup>, Michelle A. Rudek<sup>2</sup>, Christine L. Hann<sup>3</sup>, and Caren L. Freel Meyers<sup>1,\*</sup>

<sup>1</sup>Department of Pharmacology and Molecular Sciences, Johns Hopkins University School of Medicine, Baltimore, Maryland <sup>2</sup>Analytical Pharmacology Core of the Sidney Kimmel Comprehensive Cancer Center at Johns Hopkins University School of Medicine, Baltimore, MD <sup>3</sup>Department of Oncology, Johns Hopkins University School of Medicine, Baltimore, Maryland

### Abstract

Bisphosphonates are used clinically to treat disorders of calcium metabolism, hypercalcemia and osteoporosis, and malignant bone disease. Although these agents are commonly used in cancer patients and have potential direct anticancer effects, their use for the treatment of extraskelatal disease is limited as a result of poor cellular uptake. We have designed and synthesized bisphosphonamidate prodrugs that undergo intracellular activation to release the corresponding bisphosphonate and require only two enzymatic activation events to unmask multiple negative charges. We demonstrate efficient bisphosphonamidate activation and significant enhancement in anticancer activity of two bisphosphonamidate prodrugs *in vitro* compared to the parent bisphosphonate. These data suggest a novel approach to optimizing the anticancer activities of commonly used bisphosphonates.

### Keywords

bisphosphonates; clodronate; bisphosphonamidate; prodrug; lung cancer

### Introduction

Clinically used bisphosphonates (BPs) are stable analogs of naturally occurring pyrophosphate.<sup>1,2</sup> BPs are known to inhibit cancer cell adhesion and invasion, and inhibit the growth of cancer cells in the bone microenvironment.<sup>3,4</sup> The two bisphosphonate classes, nitrogen-containing (NBP) and non-nitrogen-containing (NNBP), are distinguished structurally by the substitution pattern at the bridging methylene of the P-C-P linkage (Figure 1). The NBP class incorporates a nitrogen-containing substituent at the bridging methylene (e.g. zoledronate, aledronate, pamidronate) whereas the NNBP class lacks this nitrogen-containing substituent (e.g. clodronate, etidronate).

These BP classes are further distinguished by differences in mechanism of action. The NBP class inhibits an essential enzyme in isoprenoid biosynthesis, farnesyl pyrophosphate synthase (FPPS), leading to lower FPP levels and subsequent reduction in downstream

\*725 N. Wolfe St. WBSB 305, Baltimore MD 21201. Phone: 410-502-4806. Fax: 410-955-3023. cmeyers@jhmi.edu.

**Supporting Information.** Characterization data for **14** and **15**, including NMR and HPLC; stability of **14** and **15** in media; control experiment assessing chemical conversion of prodrug **14** to derivatized bisphosphonate **18**. This material is available free of charge via the Internet at <http://pubs.acs.org>.

protein prenylation events in osteoclasts and malignant bone cells. Recent reports suggest that increased levels of the FPPS substrate, IPP, caused by inhibition of FPPS by NBPs, promote formation of AppIPP (triphosphoric acid 1-adenosine-5'yl ester 3-(3-methylbut-3-enyl) ester), which is believed to induce apoptosis.<sup>5</sup> In contrast, NNBP undergo conversion to the corresponding nonhydrolyzable ATP analogs. Clodronate is metabolized to the ATP analog AppCCl<sub>2</sub>p (adenosine 5'-β-γ-dichloromethylene triphosphosphate), which is believed to be the active metabolite responsible for the apoptotic activity of clodronate observed in osteoclasts and malignant bone cells.<sup>6,7</sup> Further, AppCCl<sub>2</sub>p was shown to inhibit mitochondrial metabolism through inhibition of ADP/ATP translocase, and it is conceivable that additional targets are susceptible to inhibition by AppCCl<sub>2</sub>p.<sup>8</sup>

Skeletal-related events (SKE) such as fracture, spinal cord compression and hypercalcemia, are common and cause of significant morbidity in cancer patients with bone metastases.<sup>9</sup> Bisphosphonate therapy has been shown to reduce the rate of SKE in several clinical trials leading to its use as a standard adjunct therapy in patients with bone metastases. The clinical success of NBPs in the prevention and management of bone metastases has led to the evaluation of BPs as potential therapeutic agents for the treatment of cancer in soft tissues.<sup>1</sup> The NBP zoledronate (**6**, Figure 1) is a commonly used BP in metastatic bone disease and exhibits varying anti-cancer activities with IC<sub>50</sub>s ranging from 3 to >100 μM in several cancer cell lines.<sup>1, 10, 11</sup> The cytotoxic effects of zoledronate in cancer cells are believed to be exerted through a variety of mechanisms, including blockage of cell cycle in models of non-small cell lung cancer,<sup>12</sup> inhibition of angiogenesis,<sup>13–16</sup> and induction of apoptosis in small cell lung cancer cell lines,<sup>11</sup> although the molecular mechanisms beyond inhibition of FPPS are not well-understood.

NNBPs, including clodronate (**2**, Figure 1) are significantly less potent anticancer agents,<sup>17</sup> exhibiting growth inhibition in the high micromolar or low millimolar range in breast and ovarian cancers,<sup>10</sup> and minimal activity against lung cancer cell lines<sup>10</sup>. The anticancer activity of clodronate is thought to correlate with formation of AppCCl<sub>2</sub>p in breast, prostate and myeloma cells<sup>18</sup>; however, the molecular mechanisms underlying the anticancer effects of clodronate are not well-understood.

BPs are polyanionic at physiologic pH, and are consequently concentrated in the mineralized bone matrix.<sup>19</sup> While beneficial for the treatment of bone disorders, this structural characteristic of BPs precludes efficient uptake into extracellular tumor cells. The low cellular uptake of BPs presents a critical barrier both for the development of these agents to treat tumors in soft tissues and for studies to elucidate the intracellular mechanisms by which BPs exert anti-tumor effects.

Existing strategies to increase bioavailability of NNBP such as clodronate have involved masking of the BP scaffold with biodegradable or chemically labile groups designed to release the corresponding BP through non-specific esterase activation or chemical hydrolysis post-intestinal absorption.<sup>20–22</sup> These prodrugs generally undergo rapid extracellular bioactivation in serum, leading to partially unmasked, impermeable intermediates, which are often inefficiently converted to the fully unmasked BP.<sup>20</sup> There are no such prodrug strategies reported for BPs bearing the tertiary hydroxyl group at the bridging methylene position, including the NBP class, owing to the intrinsic instability of these compounds when masked as tetraesters.<sup>23</sup> Other strategies to increase BP cell permeability have focused on introducing modifications at the bridging methylene of the P-C-P linkage to increase hydrophobicity. Such modifications have also been shown to impart changes in target specificity.<sup>24–26</sup> Increasing hydrophobicity of substituents at the bridging methylene group does not overcome low membrane permeability entirely, as phosphonate masking strategies have been employed in these cases as well.<sup>22, 27</sup>

Here we report a novel bisphosphonamidate prodrug strategy for the intracellular release of bisphosphonates and demonstrate its application to bisphosphonic acid and the clinically-used NNBP clodronate. Our results suggest bisphosphonamidate prodrugs undergo rapid activation to release the corresponding BP following reductive activation of nitroaryl delivery groups. Further, we demonstrate intracellular conversion of a bisphosphonamidate prodrug to the corresponding bisphosphonate, and a remarkable enhancement in anticancer activity of two bisphosphonamidate prodrugs compared to the parent bisphosphonates in A549 cells.

## Results

### Design and Synthesis of Bisphosphonamidate Prodrugs

We have designed a prodrug strategy to enhance membrane permeability of bisphosphonates through incorporation of two biodegradable nitroaryl delivery groups and two halobutyl amine masking groups, which effectively mask the polyanionic charges (Scheme 1). The bisphosphonate design shown here extends the halobutyl phosphoramidate prodrug strategy developed for the intracellular delivery of nucleotides.<sup>28</sup>

Membrane permeable bisphosphonamidate prodrugs (**7**) are designed to undergo rapid intracellular bioreduction to produce the corresponding hydroxylamine **8** (Scheme 1), which undergoes elimination through the aromatic ring and expulsion of phosphonamidate anion **9**. The resulting increase in electron density of the phosphonamide nitrogen atom facilitates a cyclization reaction to produce the corresponding zwitterionic intermediate **10**. Subsequent rapid P-N bond hydrolysis affords the unmasked phosphonate **11** in a similar manner to nucleotide release.<sup>28, 29</sup> The release of the second phosphonyl group is achieved in the same manner to give the fully unmasked bisphosphate, **12**. Although it is difficult to predict the kinetics of activation, efficient release of the fully unmasked bisphosphonate is expected. An advantage of this strategy over existing bisphosphonate prodrug strategies is the requirement of a minimal number of enzymatic bioactivation steps to unmask multiple negative charges. As with the chemical deprotection of phosphoryl ester groups, removal of the first protective group is most often rapid, while removal of the second masking group is considerably slower, as a result of increased electron density at the phosphoryl leaving group and a slower rate of elimination.<sup>30</sup> The prodrug design incorporates a single nitroaryl delivery group at each phosphonyl group that is susceptible to rapid intracellular enzymatic activation by nitroreduction. The subsequent activation steps to release the fully unmasked bisphosphonate rely only upon the intrinsic chemical reactivity of the enzymatically reduced bisphosphonamidate **8**, rather than subsequent, inefficient enzymatic activation events.

Bisphosphonamidate prodrugs were synthesized as diastereomeric mixtures (Scheme 2). Deschloro bisphosphonamidate **14** was prepared via a two-step, one-pot synthesis. *N*-Methyl-*N*-chlorobutylamine hydrochloride was prepared as previously described.<sup>31</sup> Coupling of *N*-methyl-*N*-chlorobutylamine substituents to methylenebis(phosphonic dichloride) in the presence of DIPEA was monitored using <sup>31</sup>P NMR. In a representative synthesis, complete conversion to intermediate **13** was confirmed by the disappearance of the starting methylenebis(phosphonic dichloride) at  $\delta -1.53$  ppm (relative to TPPO) and appearance of two <sup>31</sup>P resonances at  $\delta$  6.17 and 6.10 ppm (1.7:1), indicating the formation of phosphonamidate dichloride **13** as a diastereomeric mixture. Treatment of **13** with nitrobenzyl alcohol in the presence of DIPEA and a nucleophilic catalyst (DMAP) afforded bisphosphonamidate prodrug **14** as a diastereomeric mixture ( $\delta$  0.84 and 0.81 ppm, 1.3:1), along with apparent hydrolysis product (~20%). Clodronate prodrug **15** was prepared by chlorination of bisphosphonamidate **14**. In a representative synthesis, bisphosphonamidate **14** (1.5:1 mixture of diastereomers) was treated with sodium hypochlorite, resulting in a new

set of  $^{31}\text{P}$  resonances corresponding to a diastereomeric mixture of clodronate prodrug **15** ( $-9.80$  and  $-9.98$  ppm, 1:1.6).

### Confirmation of bisphosphonamidate activation

To confirm the release of a fully unmasked bisphosphonate following reduction of the bisphosphonamidate nitrobenzyl ester, bisphosphonamidate prodrug **14** was subjected to chemical reduction by dithionite under model physiologic conditions, and the subsequent reactions were monitored using  $^{31}\text{P}$  NMR (Figure 2). Upon solubilization and reduction of **14**, a resonance appearing at +2 ppm (relative to TPPO) was observed in the  $^{31}\text{P}$  NMR spectrum (Figure 2B). Conversion of this peak to a new resonance at  $-8.5$  ppm (Figure 2C) was observed, and is consistent with elimination and release of the bisphosphonate **1**. Confirmation of bisphosphonate release was accomplished by comparison to authentic bisphosphonate **1** (Figure 2D).

### Inhibition of cell proliferation by bisphosphonate prodrugs

Clodronate has shown little or no antiproliferative effects against multiple cells lines, due in part to low membrane permeability. Bisphosphonates **14** and **15** are fully masked and are expected to have increased cell permeability. As predicted, both **14** and **15** exhibit potent activity against A549 NSCLC cells in vitro (Figure 3) as determined by the MTS cell proliferation assay. Dose-response curves were generated using drug concentrations ranging from  $0.2\ \mu\text{M}$  to  $300\ \mu\text{M}$  and cell proliferation was measured at 24, 48 and 72 hours after drug treatment (Figure 3, Table 1). Consistent with published reports<sup>10</sup>, clodronate does not exhibit a detectable growth inhibitory effect at concentrations up to  $1\ \text{mM}$  against the growth of A549 cells. In contrast, clodronate prodrug **15** and bisphosphonate prodrug **14** exhibit remarkably enhanced activity with  $\text{IC}_{50}$  values of  $4.4 \pm 2\ \mu\text{M}$  and  $13 \pm 1\ \mu\text{M}$ , respectively, at 72 h (Figure 3A,B). While it is possible the diastereomers of **14** and **15** may be activated at different rates, they release the same achiral bisphosphonate, and comparable antiproliferative activities are observed with different diastereomeric mixtures (data not shown).

### Permeability and intracellular activation of prodrug **14**

The enhanced activity of prodrugs **14** and **15** against A549 cells (Figure 3) is consistent with increased cell permeability of these analogs. To provide further evidence that bisphosphonamidates are cell permeable, intracellular levels of prodrug **14** were measured in A549 cells treated with prodrug at varying concentrations ( $0$ ,  $10$  or  $30\ \mu\text{M}$ ) for 8 hours. As expected, LC-MS-MS analysis of cell lysate in each case indicates reasonably high intracellular prodrug levels are achieved in a concentration-dependent manner, with  $68.6$  and  $169.3\ \text{ng}/10^4$  cells **14** detected in cells treated with  $10\ \mu\text{M}$  and  $30\ \mu\text{M}$  **14**, respectively (Figure 4A).

Bisphosphonamidate **14** is designed to undergo intracellular activation to release the corresponding bisphosphonate **1**. Direct detection of intracellular bisphosphonate by mass spectrometry is difficult as these highly polar compounds have low ionization efficiency. Thus, chemical derivatization of bisphosphonate released intracellularly was carried out in an effort to provide evidence for intracellular prodrug activation. *N-t*-Butyldimethylsilyl-*N*-methyltrifluoroacetamide (MTBSTFA) has been used successfully to derivatize polar functional groups, including carboxylic acids, for mass spectrometry analysis.<sup>32,33</sup> MTBSTFA has also been used as a derivatizing agent for the detection of phosphonate-bearing 2-(phosphonomethyl)-pentanedioic acid (2-PMPA).<sup>34</sup> Thus, we have used MTBSTFA as derivatization agent for the qualitative detection of **1** released from prodrug **14** intracellularly. The presence of intracellular bisphosphonate **1** in A549 cells treated for 8 hours with prodrug **14** ( $10\ \mu\text{M}$  or  $30\ \mu\text{M}$ ) or bisphosphonate **1** ( $30\ \mu\text{M}$ ) was confirmed by

detection of the corresponding tetra-silylated derivative **18** formed following treatment of cell lysate with MTBSTFA. Indeed, tetra-silyl bisphosphonate **18** was detected in A549 cells treated with bisphosphonamidate **14** and at considerably lower levels in cells treated with free bisphosphonate **1** at a comparable concentration (Figure 4B).

### Cell viability

In order to correlate the growth inhibitory effects of **14** and **15** with cell viability, absolute cell number at varying drug concentration was determined using a trypan blue exclusion assay. The number of viable cells at each dose was determined at 0, 24, 48 and 72 hours following drug treatment and plotted as a percent of control (Figure 5A). The EC<sub>50</sub> of **15** determined at 48 h is  $19 \pm 4 \mu\text{M}$ , ~3.6 fold higher than its IC<sub>50</sub> determined by the MTS assay (Table 1). A similar difference in the effects of **15** on cell viability versus inhibition of proliferation was observed after a 72 hour drug treatment. Interestingly, at 24 h, cell viability was reduced by only 57% at the highest drug concentration tested; therefore an EC<sub>50</sub> was not determined. In parallel, viable cells were stained with crystal violet at 72 h following drug treatment to further demonstrate the marked reduction in cell viability upon treatment with clodronate prodrug **15** (Figure 5B). In order to confirm this reduction in cell viability, cells treated with **15** for 72 h (at 10, 30, 100 and 300  $\mu\text{M}$ ) were washed to remove the prodrug and fresh media without drug was added. Cells were then allowed to grow for an additional 48 h. No new cell growth was observed in wells containing cells treated with **15** (data not shown). Prodrug **14** affects cell viability in a similar manner with an EC<sub>50</sub> at 48 h that is ~1.6 fold greater than its IC<sub>50</sub> determined using the MTS assay.

### Cell Cycle

PI and flow cytometry analysis were performed to study the effects of prodrug **15** on cell cycle. Cell cycle analysis of cells treated with 0, 3, 10 or 30  $\mu\text{M}$  **15** for 72 h suggested cell cycle arrest with low micromolar concentrations of **15**. Unequivocal support of G<sub>1</sub> cell cycle arrest was obtained through flow cytometry analysis of cells treated with 0, 3, or 10  $\mu\text{M}$  **15** for 72 h, and with nocodazole treatment for the last 24 h of prodrug exposure. Nocodazole is a microtubulin polymerization inhibitor, known to cause G<sub>2</sub> cell cycle arrest. In the absence of prodrug **15**, nocodazole-induced G<sub>2</sub> arrest is evident (Figure 6B). However, in the presence of prodrug, a marked accumulation of cells in G<sub>1</sub> is observed as low as 3  $\mu\text{M}$ , indicating G<sub>1</sub> cell cycle arrest caused by prodrug **15**.

## Discussion and Conclusions

The poor cellular uptake of bisphosphonates into soft tissues has limited their use in the treatment of extraskelatal diseases and detailed studies to elucidate the molecular mechanisms underlying the anticancer activity of this compound class. We sought to develop a more efficient strategy for the intracellular delivery of bisphosphonates in order to realize the potential of this clinically-used compound class for the treatment of extraskelatal tumors. The bisphosphonamidate prodrugs described here is designed to be more membrane permeable than the corresponding free bisphosphonates and undergo efficient bioreductive activation to release either bisphosphonate or clodronate intracellularly. A bisphosphonamidate prodrug was rapidly activated to the corresponding bisphosphonate under model physiological conditions following chemical reduction of the nitroaryl delivery groups. Formation of free bisphosphonate as the only product is consistent with an activation mechanism that takes place via elimination, cyclization and P-N bond hydrolysis (Figure 2). As no other bisphosphonate ester intermediates were observed in the <sup>31</sup>P NMR spectrum, P-N bond hydrolysis prior to C-O cleavage is an unlikely activation pathway.

In this study, clodronate and bisphosphonate exhibited minimal activity against A549 cells up to 1 mM. The bisphosphonamidate prodrugs described here exhibit > 250-fold increase in growth inhibitory activity against A549 cells, compared to the free bisphosphonates. This remarkable enhancement in potency is presumably due to increased cell permeability of the prodrug, which allows for a substantial increase in intracellular bisphosphonate concentration. The LC-MS-MS detection of reasonably high intracellular prodrug concentrations together with the observation that bisphosphonate is released intracellularly support this idea. However, cytotoxicity of the prodrug itself cannot be ruled out as a contributing factor in the observed activity of these prodrugs. A partial growth inhibitory effect of the clodronate prodrug on A549 cells is observed as early as 24 h, and complete growth inhibition by the prodrug is observed by 48 and 72 h. The observed partial growth inhibitory effect at 24 h may reflect the dependence upon prodrug activation to release the corresponding bisphosphonate, the conversion of bisphosphonate to its active metabolite (AppCH<sub>2</sub>p or AppCCl<sub>2</sub>p), and subsequent action of these metabolites on cellular target(s). T4 RNA ligase has been shown to effectively convert NNBP to their ATP analogs.<sup>35</sup> Both bisphosphonate and clodronate are known to be substrates of T4 RNA ligase with clodronate being converted to AppCCl<sub>2</sub>p more efficiently than the corresponding conversion of the non-chlorinated bisphosphonate to AppCH<sub>2</sub>p. On this basis, we anticipate intracellular conversion of bisphosphonate to AppCH<sub>2</sub>p is also less efficient than the conversion of clodronate to AppCCl<sub>2</sub>p. The observed 3-fold decrease in IC<sub>50</sub> of **14** compared to **15** is consistent with this idea. Detailed studies to determine the kinetics of intracellular prodrug activation and clodronate metabolism are required to correlate these events with observed growth inhibitory activity.

To provide further evidence for the anticancer activity of bisphosphonamidate prodrugs **14** and **15**, a complementary assay was performed to evaluate the effects of the bisphosphonamidate prodrugs on cell viability. Cell number was determined at each dose at 24, 48 and 72 h. Interestingly, **15** decreases the viability of A549 cells to just above 50% of control at higher doses over 24 h. However, a more pronounced effect on cell proliferation was observed at 24 h in the MTS assay. The difference between antiproliferative activity and effects on cell viability at 24 h suggests that **14** and **15** exert effects on metabolic activity, which leads to cell death over time. Taken together with the observation that somewhat higher prodrug concentrations are required for effects on cell viability, these results are consistent with a mechanism of action involving prodrug activation to the corresponding bisphosphonate and subsequent conversion to the non-hydrolyzable ATP analog.

The more potent clodronate prodrug **15** was selected for cell cycle analysis studies. PI and flow cytometry analysis of A549 cells treated with the clodronate prodrug over 72 h suggested G<sub>1</sub> cell cycle arrest of A549 cells at low concentrations of prodrug **15**. G<sub>1</sub> cell cycle arrest was unequivocally confirmed in nocodazole-treated cells where an obvious shift from nocodazole-induced G<sub>2</sub> arrest to G<sub>1</sub> arrest occurred in the low micromolar range of prodrug **15**. G<sub>1</sub> cell cycle arrest correlates with the antiproliferative activity of this compound, suggesting prodrug **15** affects mitochondrial function, which leads to cell cycle arrest and eventually cell death.

The low membrane permeability of bisphosphonates imposes a significant barrier to the development of these agents for the treatment of extraskeletal tumors. Clodronate displays varying effects in different cancer cell types<sup>10</sup>, with minimal activity against lung cancer cells. Studies to investigate differences in the mechanism of clodronate action that could account for these differences are also impeded by poor cellular uptake. We have developed a bisphosphonamidate prodrug strategy that significantly enhances the membrane permeability of bisphosphonates through incorporation of two biodegradable nitroaryl delivery groups and two halobutyl amine masking groups. The use of only two biodegradable delivery

groups takes advantage of the most efficient enzymatic activation steps and exploits the exquisite reactivity of chemically labile halobutyl phosphoramidate anion intermediates along the prodrug activation pathway for rapid intracellular activation and release of the fully unmasked bisphosphonate. The remarkable enhancement of activity of bisphosphoramidate prodrugs in A549 cells compared to the parent BPs highlights the potential utility of this approach to extend the use of bisphosphonates beyond the treatment of skeletal diseases and presents a potential tool for investigating bisphosphonate mechanism of action.

## Experimental Procedures

All  $^{31}\text{P}$  and  $^1\text{H}$  NMR spectra were acquired on a 400 MHz Varian or Bruker NMR.  $^{31}\text{P}$  shifts were recorded in parts per million and referenced to triphenylphosphine oxide (TPPO) as the coaxial reference in either benzene or benzene- $d_6$ .  $^1\text{H}$  chemical shifts are reported in parts per million from tetramethylsilane. HMRS characterization of prodrugs was carried out at the University of Illinois Mass Spectrometry Lab using ES ionization. All reactions were carried out under argon unless otherwise noted. Methylene chloride and diisopropylethylamine were obtained from commercial sources and distilled prior to use. A549 cells were maintained in 1640 RPMI with 10% FBS, 1% pen/strep, 1% Glutamate, and 1% sodium pyruvate. *N*-Methyl-*N*-(4-chlorobutyl)amine hydrochloride was synthesized as previously described. $^{31}$  Methylene diphosphonic acid, dichloromethylenediphosphonic acid disodium salt, and nocodazole used in biological assays were obtained from commercial sources. Methylene diphosphonic acid was determined to be >95% pure by sodium hydroxide titration, determined by vendor. Dichloromethylenediphosphonic acid was submitted, by the vendor, to elemental analysis: calculated C (4.95%), found C (4.2%), and amount of water was determined to be 2% by Karl Fischer. Nocodazole was determined to be  $\geq 95\%$  pure by reverse-phase HPLC. LC-MS-MS experiments were conducted using an AB Sciex triple quadrupole TM 5500 mass-spectrometric detector (Applied Biosystems, Foster City, CA, USA). The instrument was equipped with an electrospray interface in positive ion mode, and controlled by the Analyst version 1.2 software (Applied Biosystems).

### 4-nitrobenzyl methylenebis(*N*-4-chlorobutyl-*N*-methylphosphoramidate) **14**

Methylenebis(phosphonic dichloride) (0.466 g, 1.87 mmol) and *N*-methyl-*N*-(4-chlorobutyl)amine hydrochloride (0.589 g, 3.73 mmol) were dissolved in  $\text{CH}_2\text{Cl}_2$  (7.48 mL) and cooled to  $0^\circ\text{C}$  with stirring under an Ar atmosphere. DIPEA (1.56 mL, 8.98 mmol) was added dropwise. The reaction mixture was allowed to warm to room temperature, and stirring was continued for 2h. Nitrobenzyl alcohol (1.43 g, 9.35 mmol) was added to the reaction mixture in one portion. In a separate flask under an Ar atmosphere, DMAP (0.228 mg, 1.87 mmol) was dissolved in  $\text{CH}_2\text{Cl}_2$  (0.2 mL) and DIPEA (0.782 mL, 4.49 mmol), and the resulting mixture was added dropwise to the reaction mixture at room temperature. The reaction mixture was stirred at room temperature for 4 hours.  $^{31}\text{P}$  NMR analysis of the crude reaction mixture showed a 1.3:1 diastereomeric mixture. The mixture was washed with saturated  $\text{NH}_4\text{Cl}$  ( $1 \times 2$  mL). The organic layers were combined, dried over  $\text{NaSO}_4$  and concentrated under reduced pressure. Removal of impurities by flash chromatography (1:99, MeOH/ethyl acetate) resulted in the isolation of a 1.9:1 diastereomeric mixture of **14** as a pale yellow oil, in 32 % yield. The purity of **14** was determined to be > 95% by HPLC (C<sub>18</sub> Rocket™ column). Method: 100% water to 100% acetonitrile, over 3 min. then 5 min at 100% acetonitrile. Retention time = 3.3 min.  $^{31}\text{P}$  NMR ( $\text{CDCl}_3$ )  $\delta$  1.00 and 0.88 ppm (1.9:1 mixture);  $^1\text{H}$  NMR ( $\text{CDCl}_3$ )  $\delta$  8.23 and 8.19 (d, 4H, 1:1.9 mixture); 7.61 and 7.54 (d, 4H, 1:1.9 mixture); 5.21 and 5.19 (m, 4H, 1:1.9 mixture); 4.94 (m, 2H); 3.56 (m, 4H); 3.25 and 3.15 (m, 2H, 1.9:1 mixture); 2.97 (m, 2H); 2.68 and 2.65 (d, 6H, 1.9:1 mixture); 2.51 and

2.41 (t, 2H, diastereotopic), 1.73 (m, 8H). HRMS: calcd. For  $C_{25}H_{37}N_4O_8P_2Cl_2$ :  $m/z$  653.1464  $[M+H]^+$ ; Found: 653.1467.

#### 4-nitrobenzyl dichloromethylenebis(N-4-chlorobutyl-N-methylphosphonamidate) **15**

Bisphosphonamidate **14** (0.350g, 0.536 mmol) was dissolved in  $CCl_4$  (1.2 mL) and MeOH (0.6 mL). Benzyltriethylammonium chloride (.054 g, 0.236 mmol) was added in one portion. 10% NaOCl solution (1.8 mL) was added with stirring. The reaction was monitored by  $^{31}P$  NMR over a period of 4 hours until completion.  $^{31}P$  NMR analysis of the crude reaction mixture showed a 1:1.6 diastereomeric mixture of **15**. The reaction mixture was quenched with saturated  $NH_4Cl$  solution (2 mL), and the product was extracted using  $CH_2Cl_2$  ( $2 \times 0.5$  mL). Removal of impurities by flash chromatography (100 % ethyl acetate to 5:95 MeOH/ethyl acetate) resulted in the isolation of a 1:1 diastereomeric mixture of **15** as a pale yellow oil, in 60 % yield. Purity of **15** was determined to be > 95% by HPLC (Altima  $C_{18}$  column, 250 mm  $\times$  4.6 mm I.D.). Method: 5:95 water/acetonitrile to 75% acetonitrile over 5 min, 75% acetonitrile for 5 min, 75–100% acetonitrile over 5 min, then 100% acetonitrile for 5 min. Retention time = 15.2 min. Although a diastereomeric mixture of **15** was observed by  $^{31}P$  NMR during reaction monitoring in methylene chloride as the reaction solvent, the diastereomers of purified **15** appear identical by  $^{31}P$  NMR in  $CDCl_3$ .  $^{31}P$  NMR ( $CDCl_3$ )  $\delta$  -9.46 (s);  $^1H$  NMR ( $CDCl_3$ )  $\delta$  8.25 and 8.21 (d, 4H, 1:1 mixture); 7.65 and 7.62 (d, 4H, 1:1 mixture); 5.41 (m, 2H); 5.26 (m, 2H); 3.53 (m, 4H); 3.42 (m, 2H); 3.13 (m, 2H); 2.90 and 2.86 (d, 6H, 1:1 mixture); 1.72(m, 8H). HRMS: calcd. For  $C_{25}H_{35}N_4O_8P_2Cl_4$ :  $m/z$  721.0684  $[M+H]^+$ ; Found: 721.0682.

#### $^{31}P$ NMR Detection of Prodrug Activation

A suspension of BP prodrug **14** (22 mM) was prepared with sonication in a 1:2:8 mixture of DMF/acetonitrile/cacodylate buffer (200 mM, pH 7.4) at 37 degrees, and the  $^{31}P$  chemical shift was recorded. Under these conditions, **14** appeared as a single resonance, and low signal intensity was observed due to low solubility of the prodrug under these conditions. After addition of dithionite (8 molar equiv.), signal intensity increased as a consequence of increased solubility of reduced and/or eliminated species. The reaction mixture was incubated at 37 degrees for the duration of the experiment.

#### *In vitro* Cell Proliferation Assays

Cell proliferation was determined using the CellTiter 96 Aqueous One Solution Cell Proliferation Assay MTS assay. A549 NSCLC cells were plated at  $1.5 \times 10^3$  cells per well in flat bottom 96 well plates in 99  $\mu$ L of media and allowed to adhere overnight. The drugs were serially diluted in 100% DMSO. For each drug treatment group, 1 $\mu$ L of a 100X stock solution was added to each well for a final DMSO concentration of 1%. Cells were treated for 24, 48 or 72 hours. Cells were incubated with MTS dye (20  $\mu$ L well $^{-1}$ ) for 40 min to 2 h. Absorbance at 490 nm was determined using a SpectraMax M2 (Molecular Devices) plate reader. The percent cell proliferation was calculated by converting the experimental absorbance to percentage of control, which was then plotted vs. drug concentration. The  $IC_{50}$  values were determined using a non-linear dose-response analysis in GraphPad Prism version 4.0. The  $IC_{50}$  is defined as the concentration of drug needed to cause a 50% decrease in proliferation compared to vehicle control.

#### Detection of Intracellular Prodrug and Bisphosphonate

A549 NSCLC cells were plated at  $1.3 \times 10^5$  cells per well in flat bottom 6-well plates. Cells were dosed as described above. At 8 hours following drug treatment, the media was removed, and the cells were washed with 1 mL PBS. Each well was trypsinized with 600  $\mu$ L trypsin for 3–5 min. The trypsin reaction was quenched with an equal volume of media.



The cells were transferred to a 15 mL conical and centrifuged at 1,100 rpm for 5 min. Supernatant was removed, and the cells were resuspended in 200  $\mu$ L of media. The cells were diluted 1:1 in 0.04% trypan blue and counted using a cytometer. The number of cells was determined at each drug concentration and time. The cells were then centrifuged at 1,100 rpm for 5 min. The supernatant was removed, and the cell pellets were washed 2  $\times$  with PBS. The supernatant was removed and the pellets were frozen at  $-80^{\circ}\text{C}$  until analyzed.

For detection of bisphosphonamidate prodrug **14** in A549 cells treated for 8 hours, the cell pellet was suspended in 0.5 mL of deionized water, and 100  $\mu$ L of the suspension was lysed using 300  $\mu$ L of acetonitrile containing temazepam (100 ng/mL) as an internal standard. The suspension was mixed vigorously for 1 minute on a vortex-mixer, and then subjected to centrifugation at  $1200 \times g$  for 10 minutes at ambient temperature. The supernatant (10  $\mu$ L) was injected into the LC-MS-MS instrument using an autosampling device operating at room temperature. Separation was achieved on a Waters X-Terra<sup>TM</sup> C<sub>18</sub> (50 mm  $\times$  2.1 mm i.d., 3  $\mu$ m) at room temperature using isocratic elution with acetonitrile/water mobile phase (60:40, v/v) containing 0.1% formic acid at a flow rate of 0.2 mL/min. Prodrug detection was performed using electrospray tandem mass spectrometry operating in positive ion mode by monitoring the ion transitions from  $m/z$  653.0  $\rightarrow$  532.0 (BP prodrug) and  $m/z$  301.2  $\rightarrow$  255.1 (temazepam). Samples were quantitated over the assay range of 2 to 1000 ng/mL. Samples were then quantitated in ng/ $10^4$  cells as: nominal concentration (ng/mL)  $\times$  5 (standardized dilution)/total number of cells (expressed as  $10^4$ ).

For qualitative detection of intracellular bisphosphonate **1** in A549 cells treated for 8 hours with prodrug **14** or bisphosphonate **1**, the cell pellet suspension was prepared as described above. Cell lysis was achieved by addition of 300  $\mu$ L of acetonitrile to 100  $\mu$ L of the cell suspension and 1000 ng/mL of 2-(phosphonomethyl)-pentanedioic acid (2-PMPA) as an internal standard. The suspension was mixed vigorously for 1 minute on a vortex-mixer, and then subjected to centrifugation at  $1200 \times g$  for 10 minutes at ambient temperature. A volume of 300  $\mu$ L of the supernatant was transferred to a glass test tube and evaporated to dryness under nitrogen at  $40^{\circ}\text{C}$ . Acetonitrile (100  $\mu$ L) was added to the residue along with 100  $\mu$ L of *N*-*t*-butyldimethylsilyl-*N*-methyltrifluoroacetamide (MTBSTFA). The mixture was subjected to vortex-mixing prior to and every 15 minutes during a 1 hour incubation at  $80^{\circ}\text{C}$ . After 1 hour, the solution was cooled to room temperature and diluted in acetonitrile (1:5, v/v) prior to injection (10  $\mu$ L) into the LC-MS-MS instrument using an autosampling device operating at room temperature. Separation was achieved on a Waters X-Terra<sup>TM</sup> C<sub>18</sub> (50 mm  $\times$  2.1 mm i.d., 3  $\mu$ m) at room temperature using isocratic elution with acetonitrile/water mobile phase (70:30, v/v) containing 0.1% formic acid at a flow rate of 0.2 mL/min. Detection of tetra-silyl bisphosphonate **18** was performed using electrospray tandem mass spectrometry operating in positive ion mode by monitoring the ion transitions from  $m/z$  633.4  $\rightarrow$  617.0 (derivatized bisphosphonate **18**) and  $m/z$  683.0  $\rightarrow$  551.4 (derivatized 2-PMPA).

### Cell Cycle Analysis

Cell cycle distribution was determined using flow cytometry. A549 NSCLC cells were plated at  $6.7 \times 10^4$  cells per well in flat bottom 6-well plates. Cells were dosed as described above. At 24, 48 or 72 hours following drug treatment, the media was collected, and the cells were washed with 1 mL PBS. Each well was trypsinized with 600  $\mu$ L trypsin for 3–5 min. The trypsin reaction was quenched with an equal volume of media. All supernatants and washes were combined and centrifuged at 1,500 rpm for 5 min. Supernatant was decanted, and the cells were washed with 2 mL 1% FBS /PBS. Cells were centrifuged at 1,500 rpm for 5 min, and the supernatant was decanted. Cells were resuspended in 1 mL cold PBS, fixed in 9 mL cold 70% ethanol and incubated at  $4^{\circ}\text{C}$  for at least 30 min. Cells

were centrifuged at 1,500 rpm for 5 min, washed with 1%FBS/PBS, and resuspended in 1 mL of 2:1 1%FBS in PBS / phosphate citric acid buffer (pH 7.8). Cells were incubated at rt for 5 min, then spun at 1,500 rpm for 5 min. The supernatant was decanted, the cells were resuspended and incubated in 300  $\mu$ L PBS/FBS/PI/RNase solution (10  $\mu$ g/mL propidium iodide and 3 K.U. of RNase A) for 30 min at 37°C. Flow cytometry was performed to analyze DNA content, collecting ten thousand PI positive gated events per sample.

### ***In vitro* Cell Count**

A549 NSCLC cells were plated at  $1.7 \times 10^4$  cells per well in flat bottom 12-well plates. Cells were dosed as described above. At 24, 48 or 72 hours following drug treatment, the media was collected, and the cells were washed with 200  $\mu$ L PBS. Each well was trypsinized with 200  $\mu$ L trypsin for 3–5 min. The trypsin reaction was quenched with an equal volume of media. All supernatants and washes were combined and spun at 1,500 rpm for 5 min. Supernatant was decanted, and the cells were resuspended in 200  $\mu$ L media. The cells were diluted 1:1 in 0.04% trypan blue and counted using a cytometer. The absolute number of cells was determined at each drug concentration. The cell number for each concentration was converted to percent of control for each time point, and plotted using GraphPad Prism 4.0. The EC<sub>50</sub> was calculated as the concentration of drug that caused a 50% decrease in number of cells compared to control.

### **Crystal Violet Assay**

A549 NSCLC cells were plated at  $1.7 \times 10^4$  cells per well in flat bottom 6-well plates. Cells were dosed as described above. Cells were analyzed at 24, 48 and 72 hours. The media was removed, and the cells were washed twice with PBS. The cells were then stained with crystal violet solution (1 mLwell<sup>-1</sup>, 0.5% crystal violet in 95% EtOH) for 5 to 15 min. The stain was removed, and the plates were rinsed with cold water and dried at room temperature.

### **Supplementary Material**

Refer to Web version on PubMed Central for supplementary material.

### **Abbreviations**

<b>BP</b>	bisphosphonates
<b>NBP</b>	nitrogen-containing bisphosphonates
<b>NNBP</b>	non-nitrogen containing bisphosphonates
<b>SCLC</b>	small cell lung cancer
<b>NSCLC</b>	non-small cell lung cancer
<b>FPP</b>	farnesyl pyrophosphate
<b>FPPS</b>	farnesyl pyrophosphate synthase
<b>SKE</b>	skeletal related events

### **Acknowledgments**

This research was supported by the Flight Attendants Medical Research Institution (FAMRI) Center for Excellence at the Johns Hopkins University School of Medicine. Mass spectrometry studies were supported by the Analytical Pharmacology Core of the Sidney Kimmel Comprehensive Cancer Center at Johns Hopkins (NIH grants P30 CA006973 and UL1 RR025005, and the Shared Instrument Grant (1S10RR026824-01)). Mass spectrometry studies were supported in part by Grant Number UL1 RR 025005 from the National Center for Research Resources

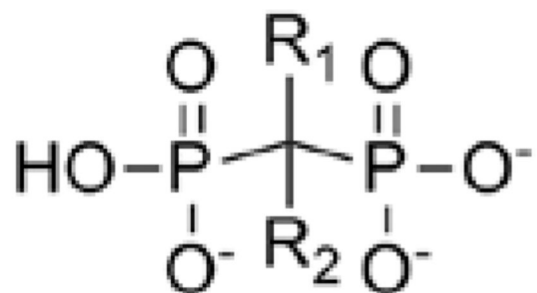
(NCRR), a component of the National Institutes of Health (NIH) and NIH Roadmap for Medical Research, and its contents are solely the responsibility of the authors and do not necessarily represent the official view of NCRR or NIH. We would like to thank Dr. Charles Rudin and Dr. Richard Borch for critical evaluation of the manuscript. We would also like to thank Dr. Timothy Burns for his contribution to the design and analysis of flow cytometry experiments.

## References

1. Morgan G, Lipton A. Antitumor Effects and Anticancer Applications of Bisphosphonates. *Seminars in Oncology*. 2010; 37(5):S30–S40. [PubMed: 21111246]
2. Gnant M. Bisphosphonates in the Prevention of Disease Recurrence: Current Results and Ongoing Trials. *Curr. Cancer Drug Targets*. 2009; 9:824–833. [PubMed: 20025570]
3. Boissier S, Magnetto S, Frappart L, Cuzin B, Ebetino FH, Delmas PD, Clezardin P. Bisphosphonates Inhibit Prostate and Breast Carcinoma Cell Adhesion to Unmineralized and Mineralized Bone Extracellular Matrices. *Cancer Res*. 1997; 57(18):3890–3894. [PubMed: 9307266]
4. Boissier S, Ferreras M, Peyruchaud O, Magnetto S, Ebetino FH, Colombel M, Delmas P, Delaissé JM, Clézardin P. Bisphosphonates Inhibit Breast and Prostate Carcinoma Cell Invasion, An Early Event in the Formation of Bone Metastases. *Cancer Res*. 2000; 60(11):2949–2954. [PubMed: 10850442]
5. Rääkkönen J, Taskinen M, Dunford JE, Mönkkönen H, Auriola S, Mönkkönen J. Correlation Between Time-Dependent Inhibition of Human Farnesyl Pyrophosphate Synthase and Blockade of Mevalonate Pathway by Nitrogen-Containing Bisphosphonates in Cultured Cells. *Biochem. Biophys. Res. Commun*. 2011; 407:663–667. [PubMed: 21420384]
6. Rogers MJ, Ji XH, Russell RGG, Blackburn GM, Williamson MP, Bayless AV, Ebetino FH, Watts DJ. Incorporation of Bisphosphonates into Adenine-Nucleotides by Amebas of the Cellular Slime-Mold *Dictyostelium-Discoideum*. *Biochem. J*. 1994; 303:303–311. [PubMed: 7945256]
7. Frith JC, Monkkonen J, Blackburn GM, Russell RGG, Rogers MJ. Clodronate and Liposome-Encapsulated Clodronate are Metabolized to a Toxic ATP analog, Adenosine 5'-(beta,gamma-dichloromethylene) triphosphate, by Mammalian Cells in vitro. *J. Bone Miner. Res*. 1997; 12(9):1358–1367. [PubMed: 9286751]
8. Lehenkari PP, Kellinsalmi M, Napankangas JP, Ylitalo KV, Monkkonen J, Rogers MJ, Azharyev A, Väänänen K. Further Insight into Mechanism of Action of Clodronate: Inhibition of Mitochondrial ADP/ATP Translocase by a Nonhydrolyzable, Adenine-Containing Metabolite. *Mol. Pharmacol*. 2002; 62:1255–1262. [PubMed: 11961144]
9. Domcheck SM, Younger J, Finkelstein DM, Seiden MV. Predictors of Skeletal Complications in Patients with Metastatic Breast Carcinoma. *Cancer*. 2000; 89:363–368. [PubMed: 10918167]
10. Knight LA, Conroy M, Fernando A, Polak M, Kurbacher CM, Cree IA. Pilot Studies of the Effect of Zoledronic Acid (Zometa) on Tumor-Derived Cells ex vivo in the ATP-Based Tumor Chemosensitivity Assay. *Anticancer Drugs*. 2005; 16(9):969–976. [PubMed: 16162973]
11. Matsumoto S, Kimura S, Segawa H, Kuroda J, Yuasa T, Sato K, Nogawa M, Tanaka F, Maekawa T, Wada H. Efficacy of the Third-Generation Bisphosphonate Zoledronic Acid Alone and Combined with Anti-Cancer Agents Against Small Cell Lung Cancer Cell Lines. *Lung Cancer*. 2005; 47(1):31–39. [PubMed: 15603852]
12. Li Y, Chang JW, Chou WC, Liaw CC, Wang HM, Huang JS, Wang CH, Yeh KY. Zoledronic Acid is Unable to Induce Apoptosis, But Slows Tumor Growth and Prolongs Survival for Non-Small-Cell Lung Cancers. *Lung Cancer*. 2008; 59(2):180–191. [PubMed: 17900752]
13. Wood J, Bonjean K, Ruetz S, Bellahcene A, Devy L, Foidart JM, Castronovo V, Gree JR. Novel Antiangiogenic Effects of the Bisphosphonate Compound Zoledronic Acid. *J. Pharmacol. Exp. Ther*. 2002; 302(3):1055–1061. [PubMed: 12183663]
14. Croucher PI, De Raeve H, Perry MJ, Hijzen A, Shipman CM, Lippitt J, Green J, Van Marck E, Van Camp B, Venderkerken K. Zoledronic Acid Treatment of 5T2MM-Bearing Mice Inhibits the Development of Myeloma Bone Disease: Evidence for Decreased Osteolysis, Tumor Burden and Angiogenesis, and Increased Survival. *J. Bone Miner. Res*. 2003; 18(3):482–492. [PubMed: 12619933]

15. Santini D, Vincenzi B, Galluzzo S, Battistoni F, Rocci L, Venditti O, Schiavon G, Angeletti S, Uzzalli F, Caraglia M, Dicuonzo G, Tonini G. Repeated Intermittent Low-Dose Therapy with Zoledronic Acid Induces an Early, Sustained, and Long-Lasting Decrease of Peripheral Vascular Endothelial Growth Factor Levels in Cancer Patients. *Clin. Cancer Res.* 2007; 13(15):4482–4486. [PubMed: 17671133]
16. Hamma-Kourbali Y, Di Benedetto M, Ledoux D, Oudar O, Leroux Y, Lecouvey M, Kraemer M. A novel Non-Containing-Nitrogen Bisphosphonate Inhibits Both in vitro and in vivo Angiogenesis. *Biochem Biophys Res Commun.* 2003; 310(3):816–823. [PubMed: 14550277]
17. Lipton A. Emerging Role of Bisphosphonates in the Clinic-Antitumor Activity and Prevention of Metastasis to Bone. *Cancer Treatment Reviews.* 2008; 34:525–530.
18. Mönkkönen H, Kuokkanen J, Holen I, Evans A, Lefley DV, Jauhiainen M, Auriola S, Mönkkönen J. Bisphosphonate-Induced ATP Analog Formation and its Effect on Inhibition of Cancer Cell Growth. *Anticancer Drugs.* 2008; 19(4):391–399. [PubMed: 18454049]
19. Russell RGG, Watts NB, Ebtino FH, Rogers MJ. Mechanisms of Action of Bisphosphonates: Similarities and Differences and Their Potential Influence on Clinical Efficacy. *Osteoporosis Int.* 2008; 19(6):733–759.
20. Ahlmark M, Vepsalainen J, Taipale H, Niemi R, Jarvinen T. Bisphosphonate Prodrugs: Synthesis and in vitro Evaluation of Novel Clodronic Acid Dianhydrides as Bioreversible Prodrugs of Clodronate. *J. Med. Chem.* 1999; 42(8):1473–1476. [PubMed: 10212134]
21. Vepsalainen J. Bisphosphonate Prodrugs. *Curr. Med. Chem.* 2002; 9:1201–1208. [PubMed: 12052172]
22. Zhang Y, Leon A, Song Y, Studer D, Haase C, Koscielski LA, Oldfield E. Activity of Nitrogen-Containing and Non-Nitrogen Containing Bisphosphonates on Tumor Cell Lines. *J. Med. Chem.* 2006; 49(9):5804–5814. [PubMed: 16970405]
23. Neimi R, Turhanen P, Vepsalainen J, Taipale H, Jarvinen T. Bisphosphonate Prodrugs: Synthesis and in vitro Evaluation of Alkyl and Acyloxymethyl Esters of Etidronic Acid as Bioreversible Prodrugs of Etidronate. *Eur. J. Pharm. Sci.* 2000; 11(2):173–180. [PubMed: 10915965]
24. Szabo CM, Matsumura Y, Fukura S, Martin MB, Sanders JM, Sengupta S, Cieslak JA, Loftus TC, Lea CR, Lee HJ, Koohang A, Coates RM, Sagami H, Oldfield E. Inhibition of Geranylgeranyl Diphosphate Synthase by Bisphosphonates and Diphosphates: A Potential Route to New Bone Antiresorption and Antiparasitic Agents. *J. Med. Chem.* 2002; 45(11):2185–2196. [PubMed: 12014956]
25. Shull LW, Wiemer AJ, Hohl RJ, Wiemer DF. Synthesis and Biological Activity of Isoprenoid Bisphosphonates. *Bioorg. Med. Chem.* 2006; 14(12):4130–4136. [PubMed: 16517172]
26. Barney RJ, Wasko BM, Dudakovic A, Hohl RJ, Wiemer DF. Synthesis and Biological Evaluation of a Series of Aromatic Bisphosphonates. *Bioorg. Med. Chem.* 2010; 18(20):7212–7220. [PubMed: 20832326]
27. Wiemer AJ, Yu JS, Shull WL, Barney RJ, Wasko BM, Lamb KM, Hohl RJ, Wiemer DF. Pivaloyloxymethyl-modified isoprenoid bisphosphonates display enhanced inhibition of cellular geranylgeranylation. *Bioorg. Med. Chem.* 2008; 16(7):3652–3660. [PubMed: 18308574]
28. Tobais SC, Borch RF. Synthesis and biological studies of novel nucleoside phosphoramidate prodrugs. *J. Med. Chem.* 2001; 44(25):4475–4480. [PubMed: 11728193]
29. Tobias SC, Borch RF. Synthesis and biological evaluation of a cytarabine phosphoramidate prodrug. *Mol. Pharm.* 2004; 1(2):112–116. [PubMed: 15832507]
30. Cox JR, Ramsay OB. Mechanisms of Nucleophilic Substitution in Phosphate Esters. *Chem. Rev.* 1964; 64(4):317–352.
31. Meyers CL, Borch RF. A Novel Method for the Preparation of Nucleoside Diphosphates. *Org. Lett.* 2001; 3(23):3765–3768. [PubMed: 11700133]
32. Prieto JA, Andrade F, Martin S, Sanjuro P, Elorz J, Aldámiz-Eschevarría L. Determination of creatine and guanidinoacetate by GC-MS study of their stability in urine at different temperatures. *Clinical Biochemistry.* 2009; 42:125–128. [PubMed: 18992235]
33. Wood PL, Khan MA, Moskai JR. Neurochemical analysis of amino acids, polyamines and carboxylic acids: GC-MS quantitation of tBDMS derivatives using ammonia positive chemical ionization. *J. of Chromatography B.* 2006; 831:313–319.

34. Yang, Wei; Laws, Katherine A.; Slecza, Bogdan; Burak, Eric S. American Association of Pharmaceutical Scientists (AAPS) Annual Meeting. Baltimore, MD 21224: Guilford Pharmaceuticals, Inc.; 1998. Development of a LC/MS/MS methods for the quantitation of 2-(phosphonomethyl)-pentanedioic acid in rat plasma and brain. Abstract # 2397
35. Sillero MAG, Diego A, Silles E, Perez-Zuniga F, Sillero A. Synthesis of Bisphosphonate Derivatives of ATP by T4 RNA Ligase. FEBS Letters. 2006; 580(24):5723–5727. [PubMed: 17010342]



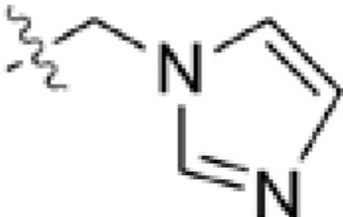
**1:**  $\text{R}_1, \text{R}_2 = \text{H}$  (Bisphosphonate)

**2:**  $\text{R}_1, \text{R}_2 = \text{Cl}$  (Clodronate)

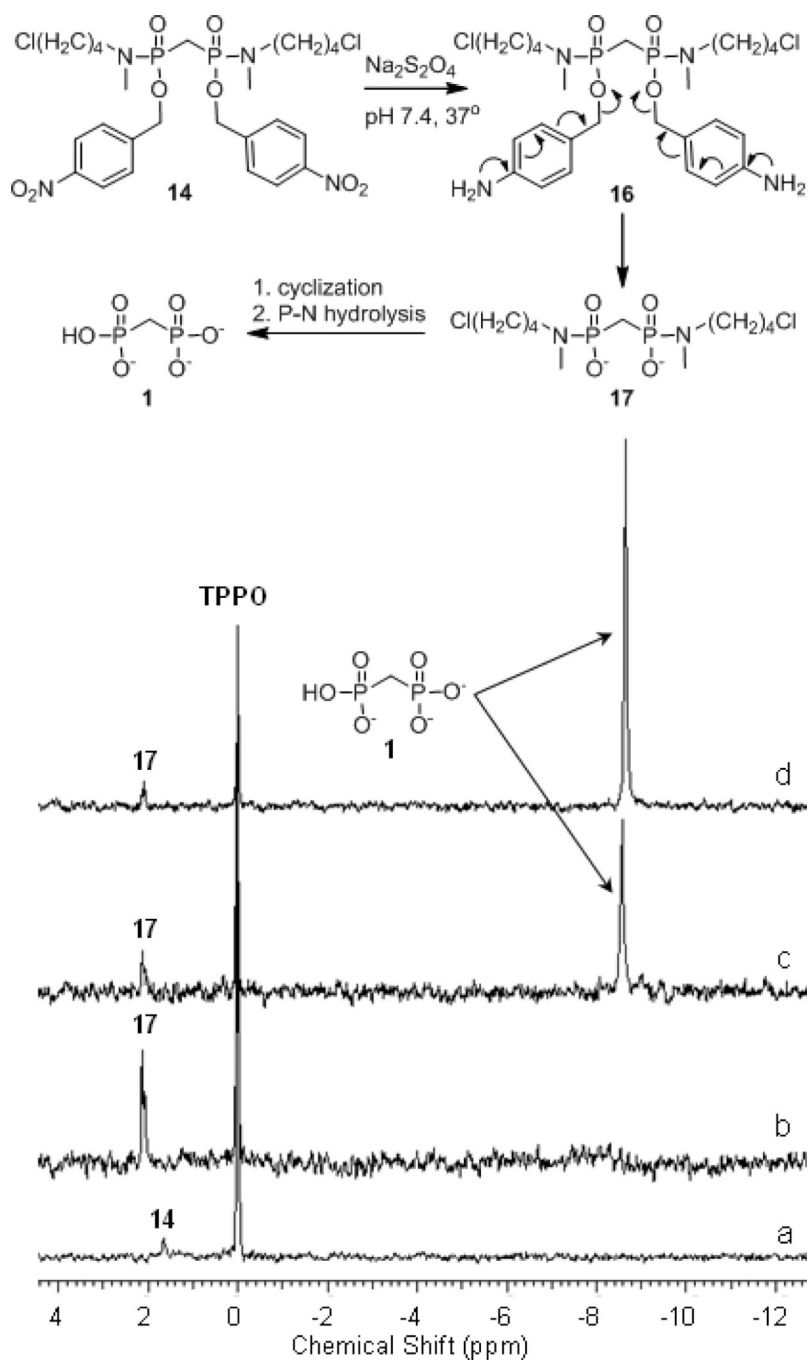
**3:**  $\text{R}_1 = \text{OH}, \text{R}_2 = \text{CH}_3$  (Etidronate)

**4:**  $\text{R}_1 = \text{OH}, \text{R}_2 = (\text{CH}_2)\text{NH}_2$  (Pamidronate)

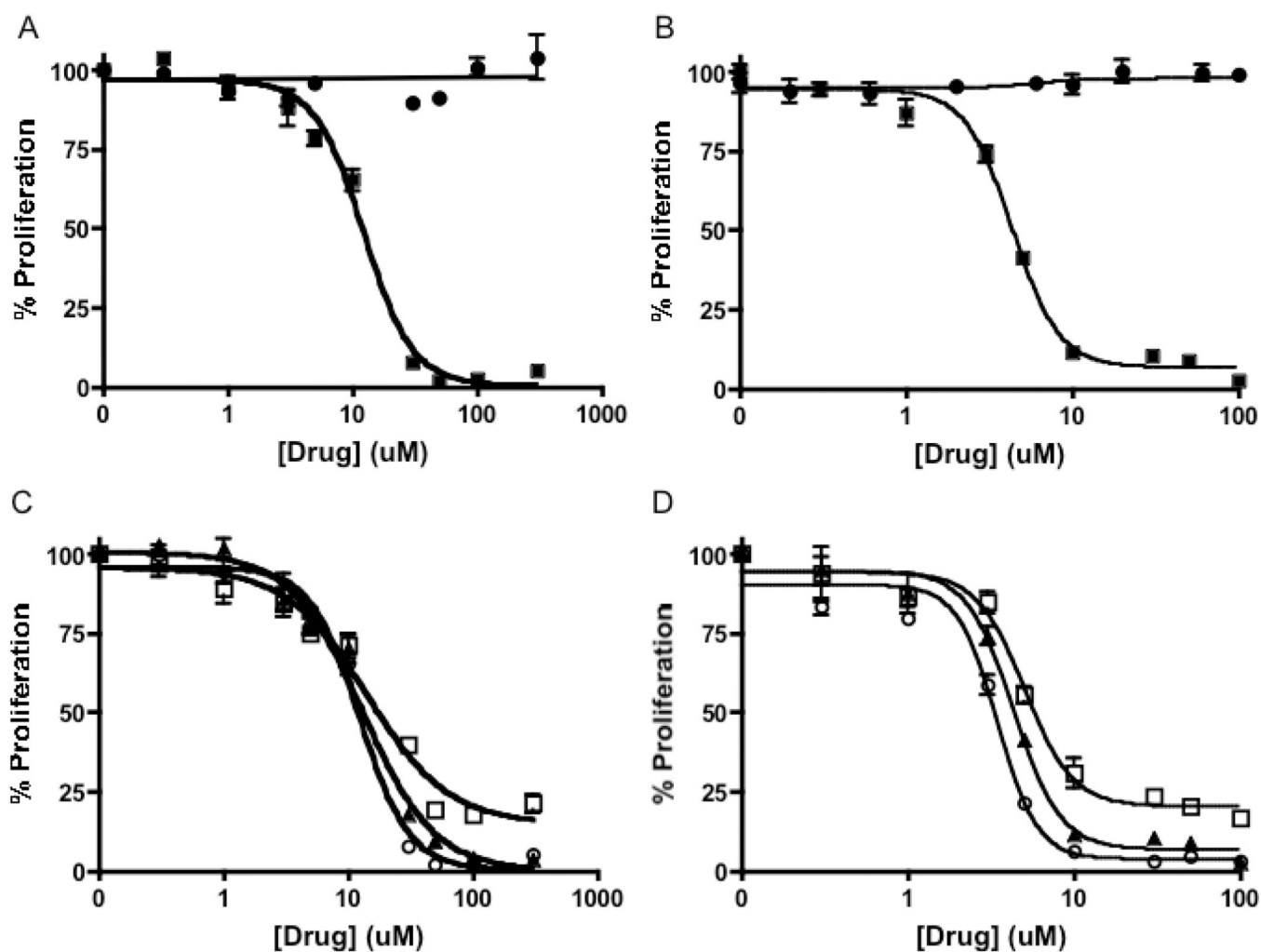
**5:**  $\text{R}_1 = \text{OH}, \text{R}_2 = (\text{CH}_2)_3\text{NH}_2$  (Alendronate)

**6:**  $\text{R}_1 = \text{OH}, \text{R}_2 =$ 

**(Zoledronate)**

**Figure 1.** Structures of nitrogen-containing bisphosphonates (NBPs) and non-nitrogen-containing bisphosphonates (NNBPs).

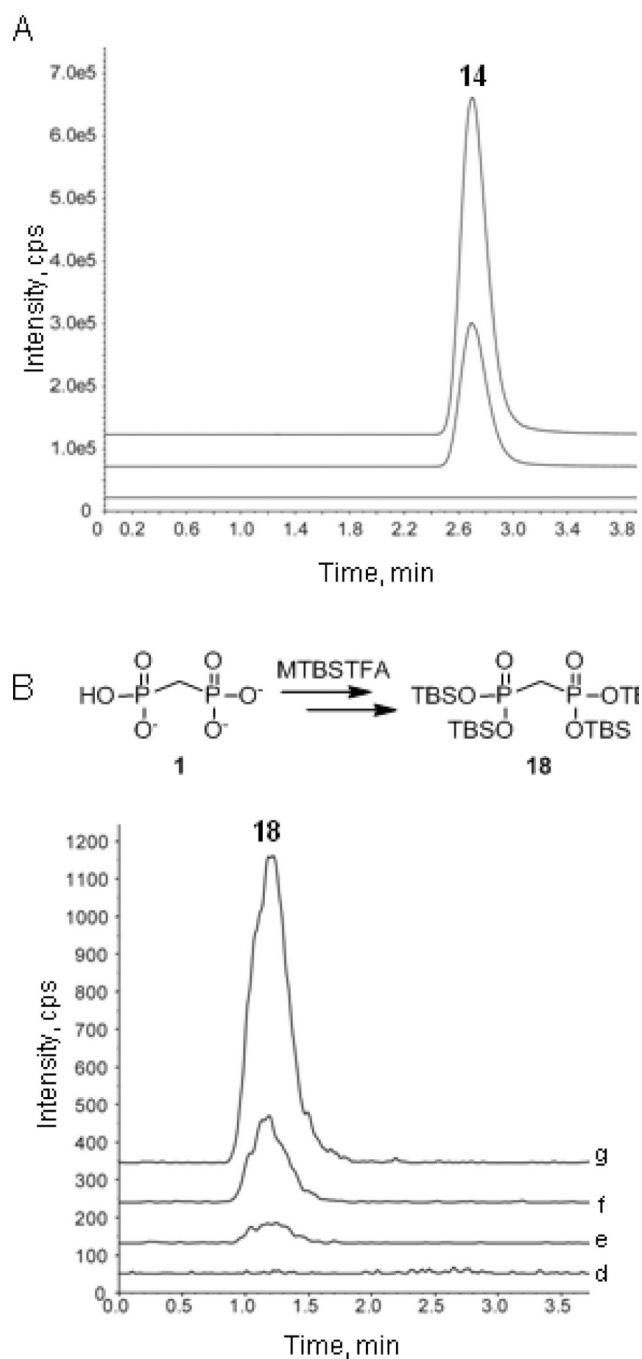


**Figure 2.** Reductive activation of BP prodrug **14**. (a) prodrug **14** prior to reduction; (b) following addition of dithionite to **14**.; (c) 4 h; (d) following addition of authentic **1** to reaction mixture shown in c.



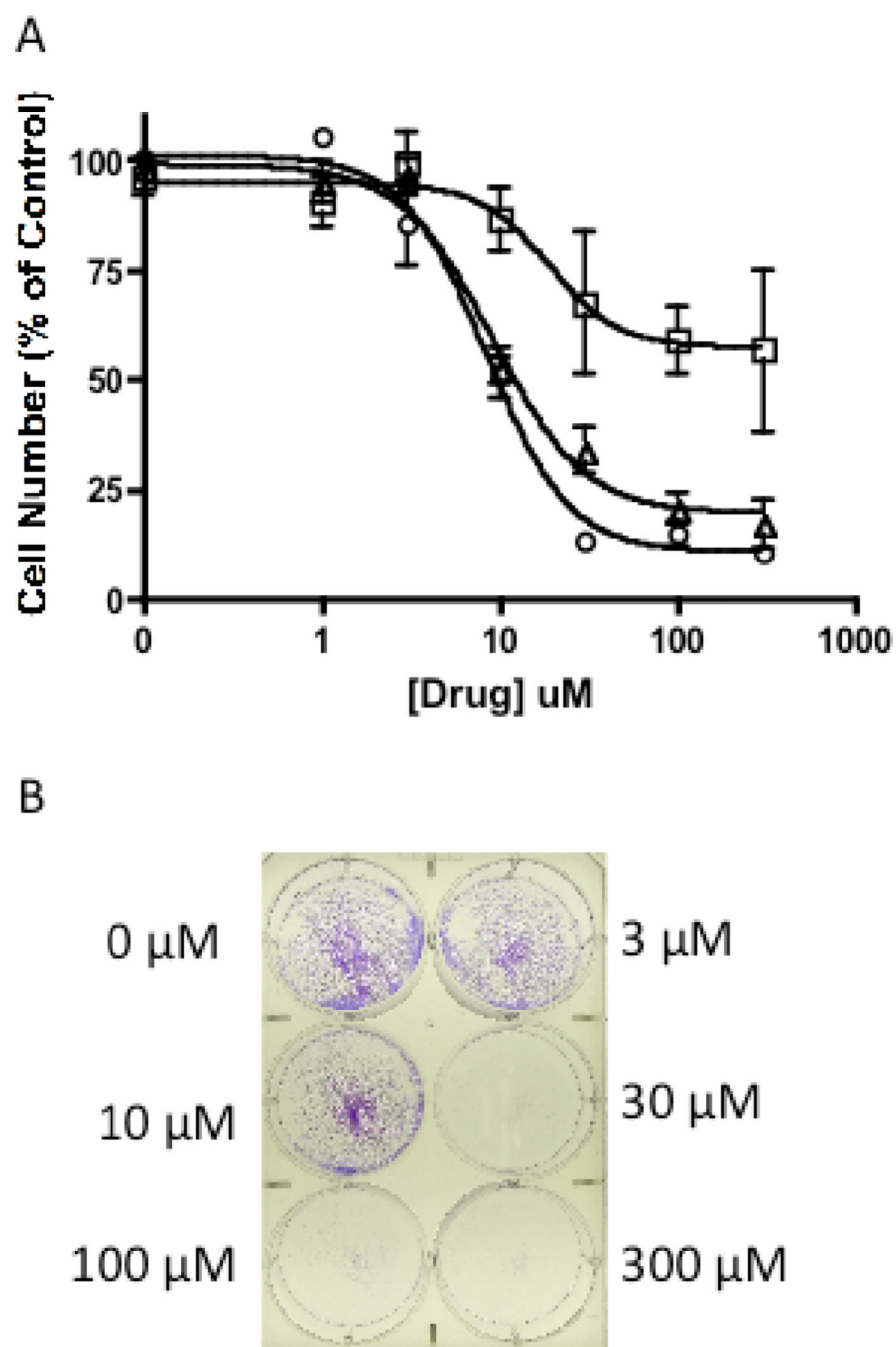
**Figure 3.** Effect of bisphosphonate prodrug **14** and clodronate prodrug **15** on proliferation of A549 cells, determined using the MTS assay. Results displayed as % of control. **A)** Bisphosphonate prodrug **14** (■) shows an enhanced anti-proliferative effect compared to bisphosphonate (●) at 72 hours. **B)** Clodronate prodrug **15** (■) shows an enhanced anti-proliferative effect compared to clodronate (●). **C)** Effect of **14** at 24 h (□), 48 h (▲), and 72 h (○). **D)** Effect of **15** at 24 h (□), 48 h (▲), and 72 h (○).



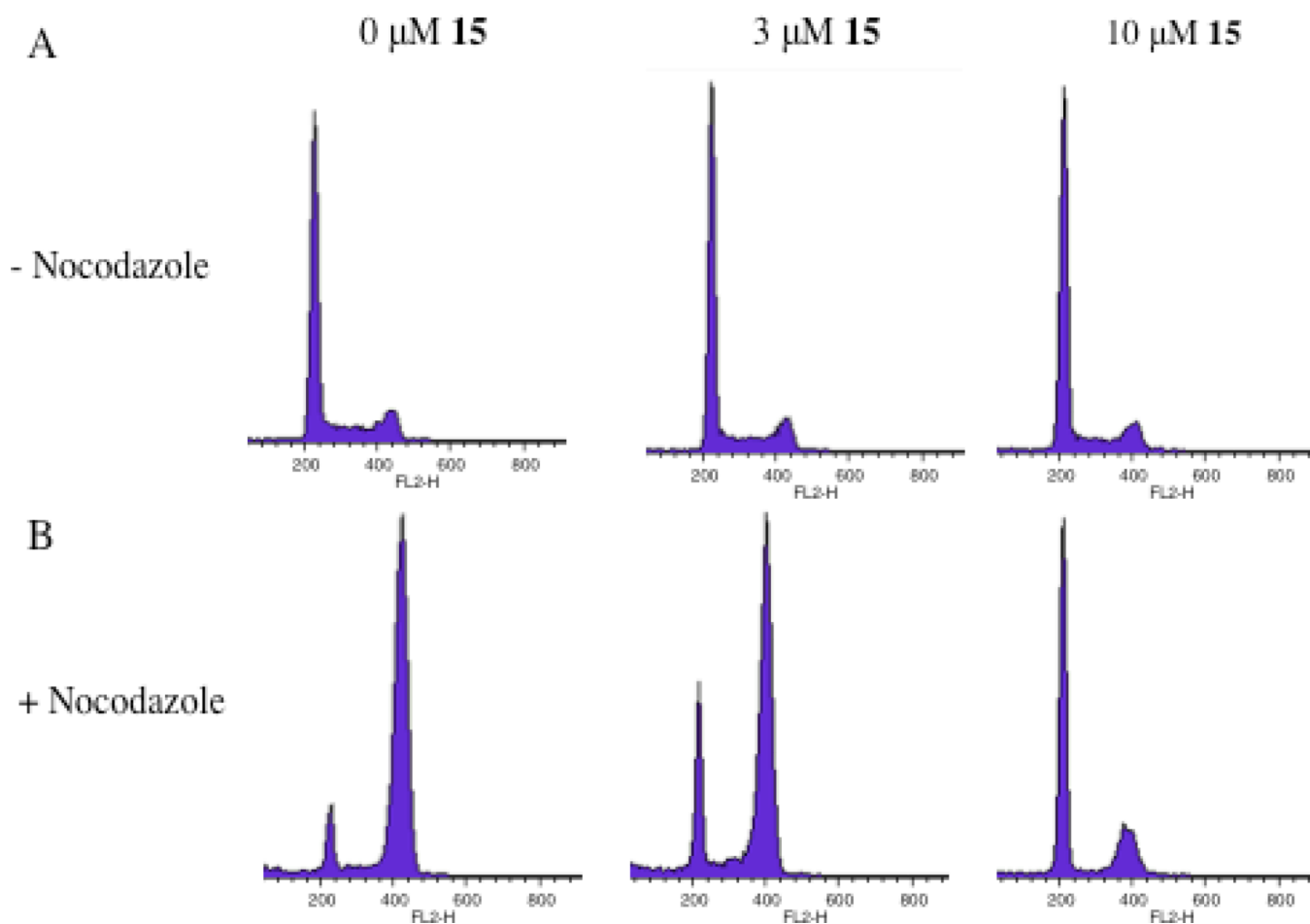


**Figure 4.**

Prodrug **14** is cell permeable (A) and undergoes intracellular activation in A549 cells to release bisphosphonate **1** (B). Figure 4A: ion chromatograms showing absence of prodrug **14** in untreated cells (a), and detection of **14** (68.6 ng/10<sup>4</sup> cells) in cells treated with 10  $\mu\text{M}$  **14** (b) and cells treated with 30  $\mu\text{M}$  **14** (169.3 ng/10<sup>4</sup> cells) (c). Figure 4B: ion chromatograms showing absence of tetra-silyl bisphosphonate **18** following MTBSTFA reaction of lysate from untreated cells (d), and detection of **18** in cells treated with 30  $\mu\text{M}$  bisphosphonate **1** (e), cells treated with 10  $\mu\text{M}$  prodrug **14** (f) and cells treated with 30  $\mu\text{M}$  prodrug **14**. Ion chromatograms are offset in the y-dimension for clarity.



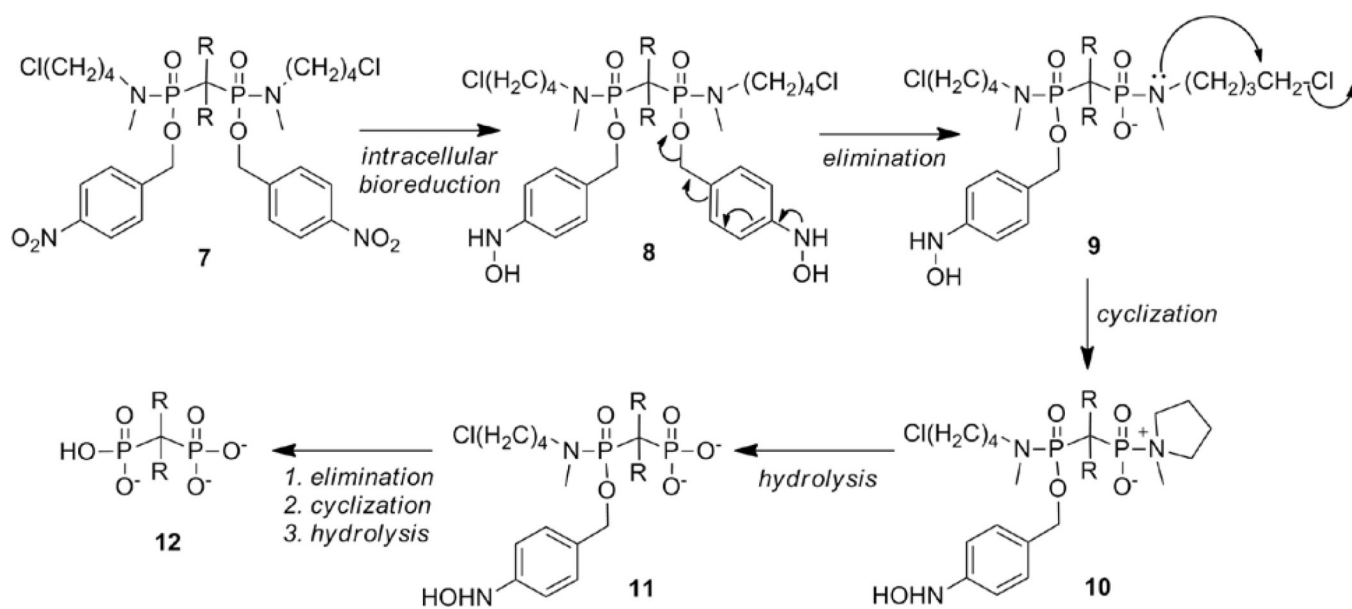
**Figure 5.** Effect of **15** on cell viability of NSCLC cells. Cell number determined using trypan blue. A) Decrease in number of NSCLC cells by **15** at 24 ( $\square$ ), 48 ( $\blacktriangle$ ), 72 ( $\bullet$ ) h. B) Crystal violet staining of A549 NSCLC cells treated with **15** for 72 h.



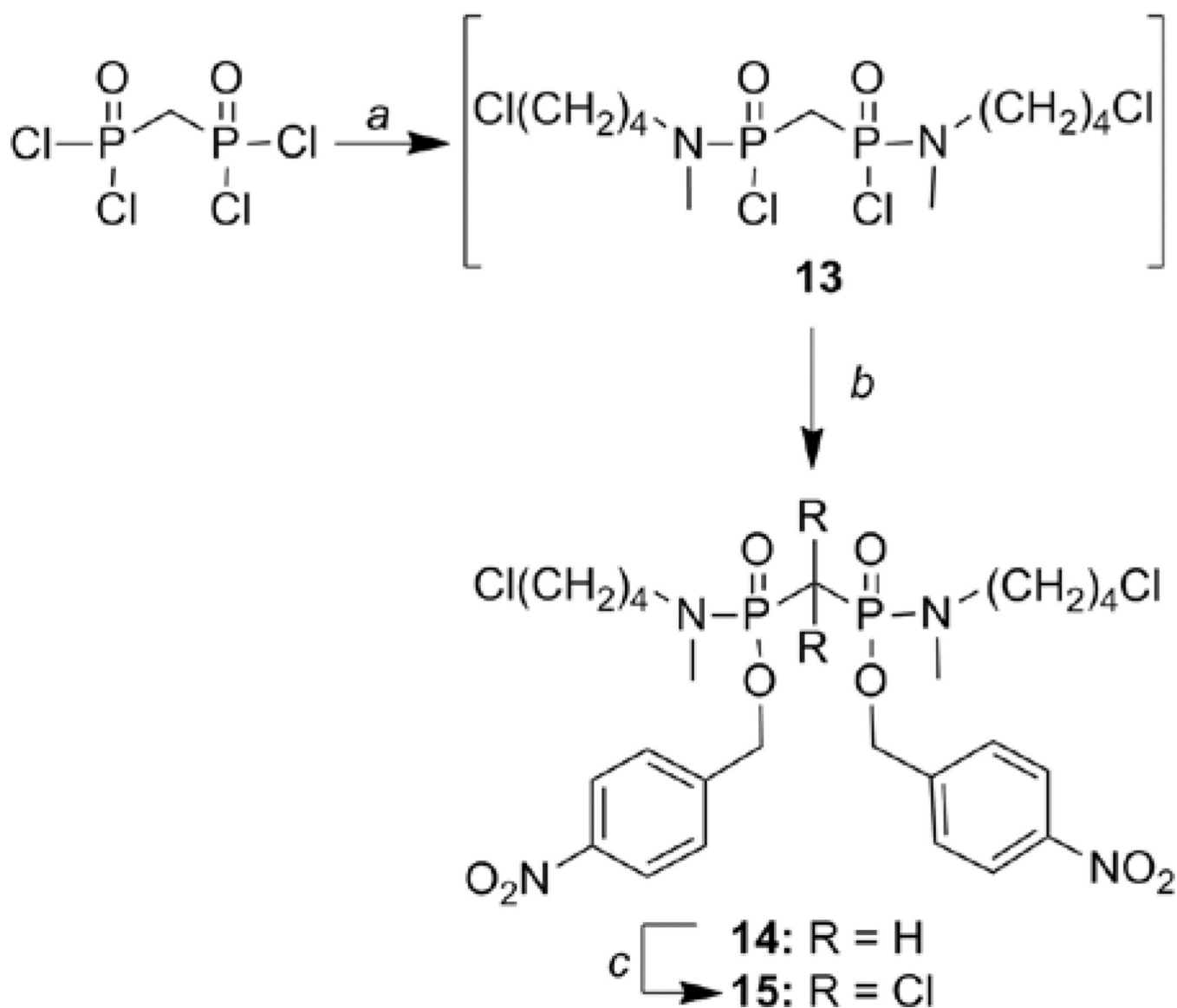
**Figure 6.**

Effect of clodronate prodrug **15** on cell cycle, determined using the PI and FACS analysis.

A) A549 cells treated with 0, 3, and 10  $\mu\text{M}$  of **15** for 72 h. B) A549 cells treated with 0, 3, and 10  $\mu\text{M}$  of **15** for 72 h and nocodazole for the final 24h. In the nocodazole-treated cells, accumulation of cells in G<sub>1</sub> phase is evident at 3 and 10  $\mu\text{M}$  of **15**.

**Scheme 1.**

Proposed intracellular bioreductive activation of bisphosphonamidate prodrugs (R = H or Cl).

**Scheme 2.**

Synthesis of prodrugs **14** and **15**. Reaction conditions: (a) *N*-Methyl-*N*-(4-chlorobutyl)amine hydrochloride, DIPEA,  $\text{CH}_2\text{Cl}_2$ ,  $0^\circ\text{C}$ ; (b) Nitrobenzyl alcohol, DIPEA, DMAP, rt.; (c) NaOCl, benzyltriethyl ammonium chloride,  $\text{CCl}_4$ , MeOH.

**Table 1***In vitro* effects of **14** and **15** on A549 NSCLC cells

Time (h)	<b>14</b>		<b>15</b>	
	IC <sub>50</sub> (μM) <sup>b</sup>	EC <sub>50</sub> (μM) <sup>c</sup>	IC <sub>50</sub> (μM) <sup>b</sup>	EC <sub>50</sub> (μM) <sup>c</sup>
24	17 ± 4	n.d. <sup>a</sup>	7.6 ± 3	n.d. <sup>a</sup>
48	15 ± 0.4	24 ± 4	5.2 ± 1	19 ± 4
72	13 ± 1	25 ± 4	4.4 ± 2	16 ± 1

<sup>a</sup>The viability of A549 cells did not decrease by 50% after 24 h of treatment with **14** or **15**.

<sup>b</sup>IC<sub>50</sub> is concentration of **14** or **15** that decreased cell proliferation by 50% compared to control.

<sup>c</sup>EC<sub>50</sub> is the concentration of **14** or **15** that decreased cell number by 50% compared to control.